

Manipulating polymer connectivity to control interfacial fracture

Mark J. Stevens

P.O. Box 5800, MS 1111, Sandia National Laboratories, Albuquerque, NM 87185-1111

(August 6, 1999)

RECEIVED

AUG 30 1999

Abstract

OSTI

By studying model polymeric networks which only differ in their connectivity, the connectivity is shown to strongly control the stress-strain response and failure modes. The sequence of molecular structural deformations that lead to failure are strongly dependent upon the network connectivity. A set of ideal, ordered networks are constructed to manipulate the deformation sequence to achieve a variety of adhesive qualities. Compared to random, dynamically formed networks, these ideal networks can be made to have either much larger or smaller failure stresses and strains. Unlike the random networks, the failure stress of an ideal network can be made close to the ideal stress equal to breaking all bonds to the substrate. By varying the number of bonds to the surface, the failure mode can be controlled to be either adhesive or cohesive.

We know quite a bit of practical information about glues, but our understanding has large gaps [1-3]. The lack of understanding primarily comes from the difficulty of treating interfaces both experimentally and theoretically. In this report, the focus is on theoretically treating the interface between a polymer network and a solid. Molecular dynamics (MD) simulations are performed to examine the role of connectivity in adhesive polymer networks such as epoxies. It is well known that the connectivity of a polymer system controls much of polymer dynamics [4]. Here, the focus is on how the connectivity of a highly crosslinked polymer network controls a variety of features in the fracture of the system. Two networks with the same strand lengths, but different connectivity are shown to have widely different

DISCLAIMER

This report was prepared as an account of work sponsored by an agency of the United States Government. Neither the United States Government nor any agency thereof, nor any of their employees, make any warranty, express or implied, or assumes any legal liability or responsibility for the accuracy, completeness, or usefulness of any information, apparatus, product, or process disclosed, or represents that its use would not infringe privately owned rights. Reference herein to any specific commercial product, process, or service by trade name, trademark, manufacturer, or otherwise does not necessarily constitute or imply its endorsement, recommendation, or favoring by the United States Government or any agency thereof. The views and opinions of authors expressed herein do not necessarily state or reflect those of the United States Government or any agency thereof.

DISCLAIMER

**Portions of this document may be illegible
in electronic image products. Images are
produced from the best available original
document.**

failure strains and stresses. In addition, the bond density at the interface determines whether failure is adhesive or cohesive.

Following a large body of work on polymeric systems [5], MD simulations are performed on a coarse-grained (i.e. bead-spring) polymer model. For focusing on the relationship between the network connectivity and the failure modes of the adhesive, the bead-spring model is ideal. A modification of the successful Kremer-Grest bead-spring model is used [6]. Polymer chains are composed of beads which interact via a Lennard-Jones (LJ) interaction with a cutoff at 2.5. All quantities will be in LJ units so that σ and ϵ represent the stress and the strain. In the Kremer-Grest work beads are bonded together by a finite-extensible nonlinear elastic (FENE) bond potential. In order to break bonds and preserve the continuity of the bond force, a breakable bond potential was created that approximates the FENE potential at the potential minimum. A quartic potential is used to create a potential with two minima.

$$U_4(r) = \begin{cases} k_4(r - r_1)(r - r_2)r^2 + U_0, & r < r_2 \\ U_0, & r \geq r_2 \end{cases} \quad (1)$$

The value of r_1 is set to match the FENE bond minimum. The second minimum at r_2 is the cutoff point. The potential parameters are: $k_4 = 1200$, $r_1 = 0.75$, $r_2 = 1.55$ and $U_0 = 34.69$. As in the FENE bond, the total bond potential includes the purely repulsive LJ interaction with a cutoff at $2^{1/6}$.

The maximum bond force is 70, and the maximum LJ force is 2.4. The scission force is then about 30 times the maximum LJ force. For atomic force-fields, the force ratio between the bond and the van der Waals forces is about 1000. However, a single bead represents several atoms and the LJ pair interaction represents multiple van der Waals pair interactions. With even just 3 atoms per bead, there are 9 pair interactions. A force ratio of order 100 in the coarse-grained model is representative of the atomic system. The ratio 30 in the present simulations is small, but by a factor of less than 10. The effect of varying bond strength requires more space than available here.

The complete system consists of a polymer network between two walls. The (111) direction (z -direction) is perpendicular to the walls. Each wall is composed of particles in two layers of an fcc lattice with nearest neighbor distance 1.204. The wall particles are bound to the fcc lattice sites by a harmonic spring with spring constant 100. The wall dimensions give the simulation cell lateral lengths, L_x and L_y . The separation distance between the innermost wall layers is L_z . The wall particles interact with the beads via the LJ potential [7], and some wall particles are bonded to the polymer network by Eq. 1. The dynamics of the system is performed at constant temperature using the Langevin thermostat [8]. The integration time step is 0.005, and the damping constants are 1 for the monomers and 5 for the walls.

The general goal is to study networks as a function of the strand length. Here, the focus is on adhesives such as epoxies which have short strands. Epoxies are chemically cured networks formed from a liquid mixture of a resin (Bisphenol A) and a crosslinker [9]. They form highly crosslinked molecular networks with each strand consists of only a few monomers. Each bead corresponds typically to 2 or 3 monomers [6]. A bead-spring model with two beads per strand was found to be the best match to epoxy data.

Two types of networks are studied in these simulations. To create a random network similar to epoxy networks, crosslinking a liquid mixture is performed dynamically. To provide a simple model for easier theoretical treatment, an ordered network is constructed. Random network formation starts with an equilibrated two component liquid mixture. The mixture consists of two bead strands and strand already bonded to a sixfold functional crosslinker bead. Bonds are formed when the separation between a crosslinker and a strand end or wall particle is less than 1.3 [6]. First, crosslinkers are bonded to the walls. Next, during a MD run, the crosslinkers are bonded to strands until at least 95% of all possible bonds are made. Zero load is maintained on the walls during the crosslinking. Afterward, the temperature is reduced below the glass transition temperature to 0.3.

The ordered network is designed to create a uniform distribution of strains. It is sixfold coordinated with two monomers between each crosslinker just as the random networks. The

network is constructed using the body centered cubic (bcc) lattice as a template (see Fig. 1(a)). Crosslinkers are the central particles in the bcc cells yielding a sixfold lattice. The z -direction is the (111) lattice direction. There are two (111) planes each with 3 sites in the bcc cell. These sites represent strands which form a zig-zag path between crosslinkers. This path is adjusted to achieve the correct density. The positions at the origin and at (1,1,1) in the bcc cell are vacant. Figure 1 shows the basic building block of the network and gives more details of the network geometry. The system is created at $\rho = 0.8$ and then equilibrated to $T = 0.3$ and zero load just as the random networks.

When a tensile pull is applied to the ordered network, the strands should straighten out uniformly like an accordian. Because the system is globally homogeneous, each strand is expected to straighten out and become taut before any bond breaking occurs. Thus, this system should expand considerably more before failure than the random structures.

The tensile pull is performed by moving the top and bottom walls apart at constant velocity. As in experiments, simulations show that the yield stress and strain increase slightly with increasing strain rate. The wall velocities are in the range 0.001–0.1 which is slow enough not to perturb molecular scale relaxations. The failure strain does not depend on the strain rate in this velocity range.

Four different random networks have been simulated. The random network R1 has about 9800 monomers and the initial dimensions are $L_x = 19.3$, $L_y = 33.1$ and $L_z = 15.1$. The system R2 has twice the plate area as R1, and R3 has twice the plate separation as R2. R4 is a ‘large’ system with about four times the area and height of R1.

In Fig. 2 the stress-strain curve of R1 is shown. R2 and R3 have almost identical curves. The yield stress is about 4 and the yield strain is 0.1. The stress drops suddenly and complete failure occurs at $\varepsilon_f = 1.0$ and $\sigma_f = 3.4$. For R1 the first bond breaks at $\varepsilon = 0.62$. Between $\varepsilon = 0.82$ and 1.0 all the bonds between the network and the bottom wall break resulting in failure.

All the R systems fail interfacially with a preceding sequence of molecular deformations. Initially, the near neighbors are plastically deformed producing the yield behavior. The

yield stress is determined by the LJ interactions and is identical for all systems. Once the monomers have moved beyond their initial local position, further applied strains tighten the strands of the network. In the plateau region, calculations of the bond length distribution show that the bonds are not stretched. Before bonds can stretch strands must be pulled taut which requires large local strains. After the strands are taut, the bonds must and do stretch. Subsequently, bonds break and the adhesive fails.

Even for dimer strands, the local strain required to bring the strands taut is large. An upper limit to the failure strain is the minimal path length P from a top wall particle bonded to the network to a bottom wall particle bonded to the network. Using Dijkstra's method [10], the average value P_{ave} for the random networks is typically about $2L_z$. Not surprising, this value indicates that the minimal paths follow a zig-zag path. For the different random systems, P_{ave} and the shortest value in terms of strain are in the range 0.85-0.90 and 1.0-1.1, respectively. For R1 the shortest path's bonds will be near breaking by a strain of at most 0.84, and by a strain of 1.1 all the paths' bonds will be near breaking. These values are consistent with the failure strain for R1. However, for the large system R4 which has similar maximum strain values, failure occurs at a much lower strain, 0.25. This size effect may indicate stress concentrations dependent on system size. The important issue of size dependence will be dealt with in forthcoming work.

As discussed above, the ordered networks are designed such that the whole system should homogeneously straighten out like an accordian become taut before any bond breaking occurs. Failure should consequently occur at much higher stains than in the random system. The stress-strain curve is shown in Fig. 2 for the ordered system O1 with one bond per crosslinker to the wall as in the random structure. The yield stress is identical to the random network's. As expected, failure occurs at a much larger strain, $\epsilon_f = 2.5$. The fully taut configuration is a zig-zag path (see Fig. 3(b)). The strain for this taut configuration at which the bonds must begin to stretch is 2.3 as calculated directly from the geometry. This value is consistent with the simulation result that the stress begins to the large rise at this strain because the bonds are being stretched. Figure 3 shows that the strands open up

as expected, yet deformation is not completely homogeneous since the system starts below the glass transition temperature. Initially, in a small region the strand expansion nucleates. This region grows with increasing strain spanning the system in the x -direction. Then, layer by layer the rest of the strands straighten out. The noticeable rises in the stress-strain curve before the final rise to failure are due to the extra stress it takes to pull the two layers at the walls. Just as in any liquid, the layers near the wall are more strongly packed, and, consequently, more force is need to pull the layers apart. Once the system is completely opened up, the bonds begin to stretch and then break at the interface. Finally, interfacial failure occurs.

Because the system has uniformly deformed, more of the bonds break simultaneously and the failure stress is larger in this case than in the random case. The ideal fracture stress is

$$\sigma_{id} = F_{br} * N_b / A \quad (2)$$

where F_{br} is the force to break a bond, N_b is the number of bonds to the wall, and A is the wall area. O1 and R1 have $N_b = 60$ and $\sigma_{id} = 6.5$. The fracture stress of O1, $\sigma_f = 4.9$ is much closer to the ideal value than R1's value (3.4). The main reason is that bonds break over a wider range of strains in R1 than O1. For R1, interfacial bond breaking occurs over a strain range of 0.18, but for O1 the range is just 0.005! Thus, at any given strain fewer bonds are broken in R1, and there is a significantly smaller contribution to the force on the walls due to bond breaking.

The reason for interfacial failure is especially clear in the O1 case. The number of bonds at the interface is fewer than the number of bonds elsewhere in the network. This occurs simply because only one bond per crosslinker is allowed to the wall when constructing the system which has some geometric merit. Figure 4 shows the number of bonds $b(z)$ near failure that cross the z -plane at z . Away from the interface, the average noninterfacial $b(z)$ is 380 for R1 and is uniformly 180 for O1. Since R1 is near failure at a much lower strain, more bonds cross a given plane due to the larger density than for O1. Yet, for these two

cases at the interface $b(z)$ remains at 60, because of the bonding constraints. Thus, for R1 and O1, fewer bonds at the interface must stretch more to apply a larger force; consequently, failure occurs at the interface.

A system, O3, was constructed identical to O1, but with three bonds per crosslinker to the wall by positioning crosslinkers above the wall particles in the middle of the triangles of the fcc layer and bonding to each particle in the triangle. In this case, the same number of bonds occurs for all crosslinkers. There should be no preference to failure at the interface. Given that the interface is a small fraction of the system, failure is likely to occur within the network—cohesively.

The bond distribution $b(z)$ for O3 given in Fig. 4 is identical to O1 near failure except at the interface where $b(z)$ matches the noninterfacial value. As a consequence, O3 fails cohesively as is clearly shown in Fig. 3(c). The stress-strain curve for O3 (Fig. 2) is similar to the O1 case. The difference is mainly that the failure stress is larger ($\sigma_f = 8.7$), but only by a factor of about two, not three like the ideal value, $\sigma_{id} = 19.5$. All the bonds break at the interface in O1 in about 1000 time steps. For O3, 6000 time steps of bond breaking occur. As noted above, this spreads the contribution of bond forces to the stress over a wider range of strains yielding a small σ_f .

Given that the accordian behavior in the ordered systems occurs with strands connecting crosslinkers in neighboring planes, creating a network with some strands connecting next nearest neighbor planes of crosslinkers should have fundamentally different behavior. An ordered system O2, was constructed that connects crosslinkers such as the two marked by X in Fig. 1. This structure results in some dangling ends at the interface, since crosslinkers at the surface do not have sites to bond to. The number of dangling ends is 60 which is similar to that for R1. The number of bonds to the walls remains 60 as in O1. The stress-strain curve (Fig. 1) exhibits failure at a *lower* strain and stress than R1. This lower strain agrees with the calculated strain $\varepsilon = 0.6$ for the taut path of connected next nearest neighbor crosslinkers. Thus, by manipulating only the network connectivity, the failure stress and strain can either be less than or greater than the random network values.

The fundamental point of this work is that the network connectivity is a critical factor controlling the nature of fracture. By creating model systems, the failure strain has been designed to be much larger or much smaller than a random, dynamically formed network. Whether failure is cohesive or adhesive depends on the number of bonds to the surface in these simulations. These model systems have been constructed based on the understanding of the sequence of molecular scale deformations that occur under tensile deformation. The key molecular deformation leading to failure is the tightening of the network strands, for the strands must be taut before bonds are stretched and break.

This work was supported by the DOE under contract DE-AC04-94AL8500. Sandia is a multiprogram laboratory operated by Sandia Corp., a Lockheed Martin Company, for the DOE.

REFERENCES

- [1] S. Wu, *Polymer Interface and Adhesion* (Marcel Dekker, New York, 1982).
- [2] R. Wool, *Polymer Interfaces: Structure and Strength* (Hanser, Munich, 1995).
- [3] H. Brown, *Science* **263**, 1411 (1994).
- [4] M. Doi and S. F. Edwards, *The Theory of Polymer Dynamics* (Oxford University, Oxford, NY, 1986).
- [5] *Monte Carlo and Molecular Dynamics Simulations in Polymer Science*, edited by K. Binder (Oxford, New York, 1995).
- [6] K. Kremer and G. Grest, in *Monte Carlo and Molecular Dynamics Simulations in Polymer Science*, edited by K. Binder (Oxford, New York, 1995), Chap. 4, pp. 194-271.
- [7] P. A. Thompson and M. O. Robbins, *Phys. Rev. A* **41**, 6830 (1990).
- [8] J. Schneider, W. Hess, and R. Klein, *J. Phys. A* **18**, 1221 (1985).
- [9] R. Morgan, F.-M. Kong, and C. M. Walkup, *Polymer* **25**, 375 (1984).
- [10] T. Hu, *Combinatorial Algorithms* (Addison-Wesley, Reading, 1982).

FIGURES

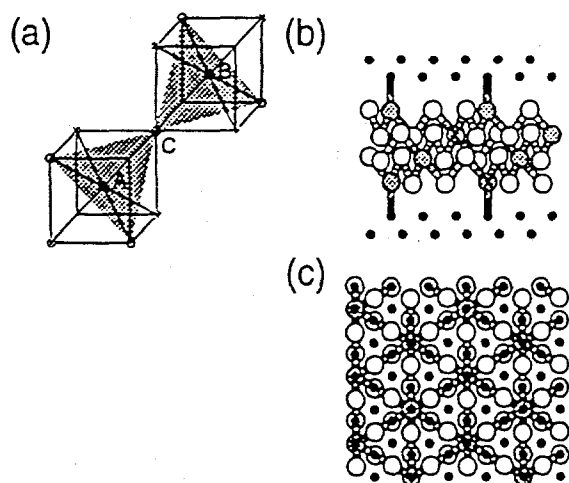


FIG. 1. The crosslinkers are positioned on layers of triangular lattices that stack in a ABC sequence. (a) In between the crosslinker planes are the strand planes (shaded region). Crosslinker A is below this strand plane and crosslinker B is above it. These two crosslinkers are bonded together through a strand at C. Parts (b) and (c) show projections of the ordered network. Part (b) shows the zig-zag path from one crosslinker (shaded) to another, and that successive layers of crosslinkers are bonded together. The Xs mark crosslinkers that are connected in system O2.

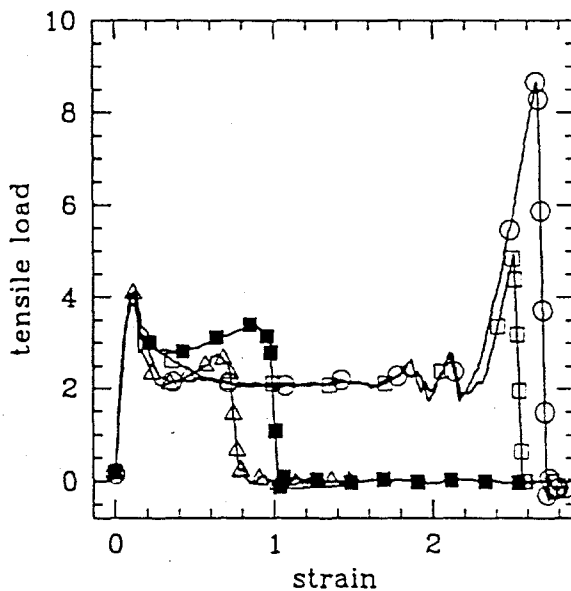


FIG. 2. The stress-strain curves for the random network R1 (solid squares) and the ordered networks O1 (squares), O2 (triangles), and O3 (circles).

FIG. 3. Images of systems under tensile strain show (a) the random, dynamically formed network R1 during failure, (b) the ordered network O1 at the same strain as (a) and (c) the ordered network O3 during failure.

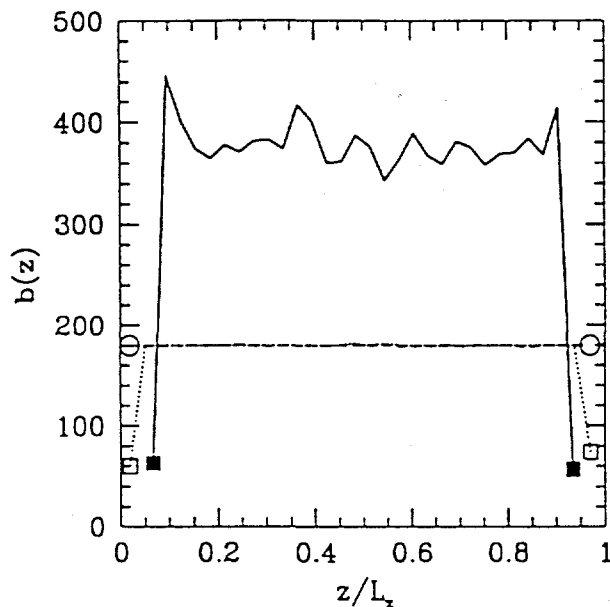


FIG. 4. The number of bonds as a function of z position show the low bond density for systems R1 (solid line) and O1 (dotted line) at the interface, and the uniform density for O3 (dashed line). The points mark the interfacial values: R1 (solid square), O1 (open square), O3 (circle).

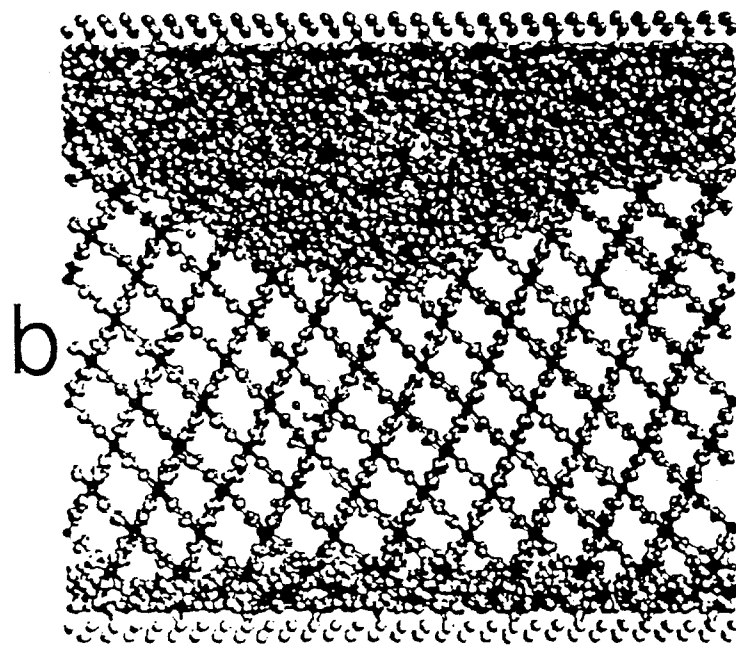
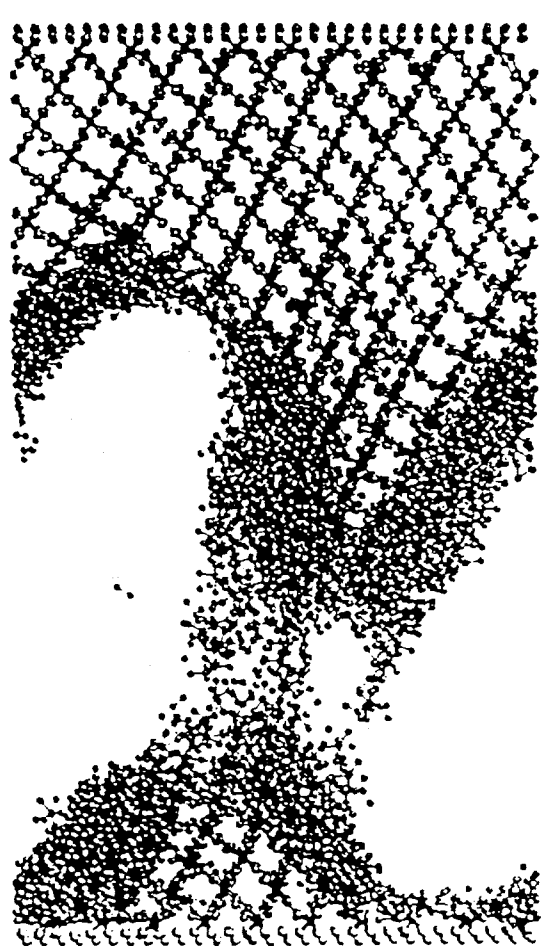
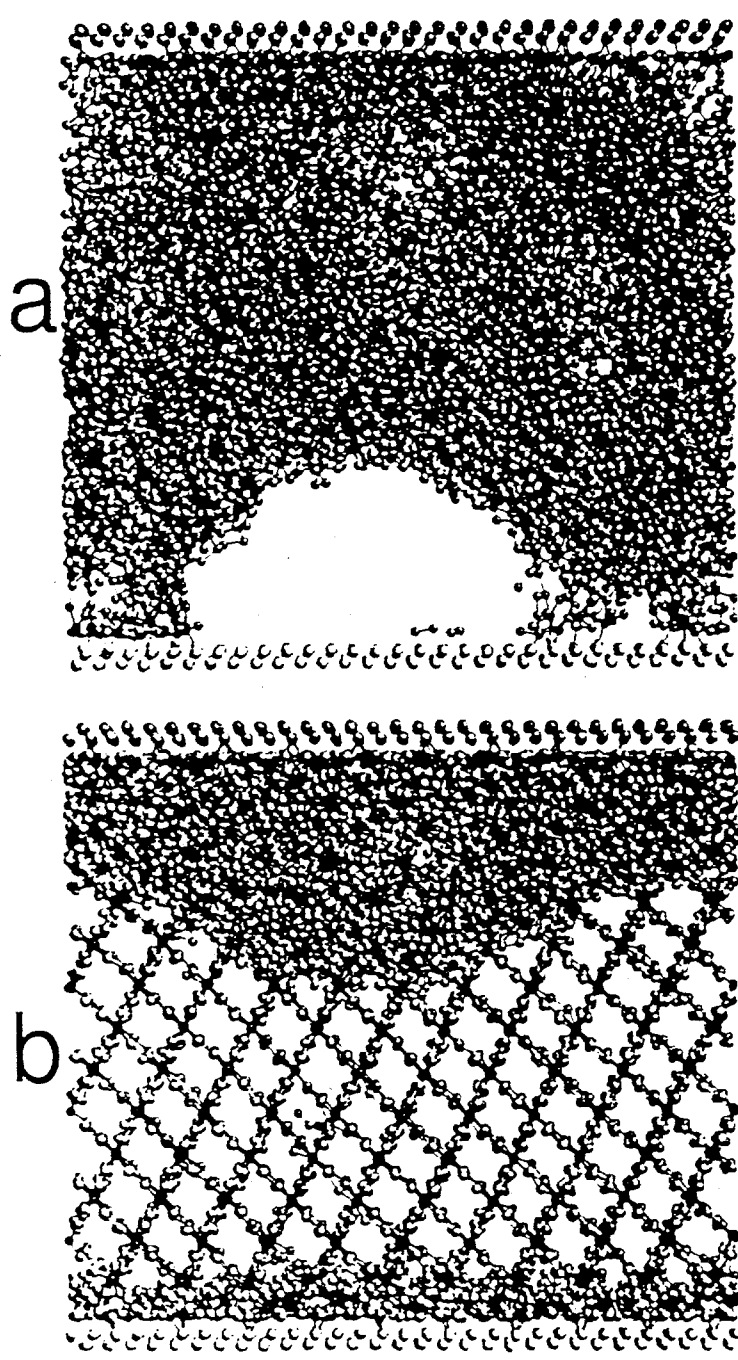


Figure 3